

## A preliminary study of the formation of $\text{WSi}_2$ by high-current W ion implantation

This article has been downloaded from IOPscience. Please scroll down to see the full text article.

1993 J. Phys.: Condens. Matter 5 5505

(<http://iopscience.iop.org/0953-8984/5/31/014>)

View [the table of contents for this issue](#), or go to the [journal homepage](#) for more

Download details:

IP Address: 171.66.16.159

The article was downloaded on 12/05/2010 at 14:16

Please note that [terms and conditions apply](#).

## A preliminary study of the formation of $\text{WSi}_2$ by high-current W ion implantation

D H Zhu<sup>†</sup>, H B Lu<sup>†</sup>, K Tao<sup>†</sup> and B X Liu<sup>††</sup>

<sup>†</sup> Department of Materials Science and Engineering, Tsinghua University, Beijing 100084, People's Republic of China

<sup>††</sup> Centre of Condensed Matter and Radiation Physics, China Centre of Advanced Science and Technology (World Laboratory), Beijing 100080, People's Republic of China

Received 14 April 1993

**Abstract.** Two differently structured  $\text{WSi}_2$  phases were formed by direct W ion implantation, for the first time, into silicon wafers using a metal vapour vacuum arc ion source. Implantation of W ions was conducted with an extract voltage of 40 kV, various beam densities from 50 to  $115 \mu\text{A cm}^{-2}$  and a fixed dose of  $5 \times 10^{17} \text{ cm}^{-2}$ . It was found that the formation of  $\text{WSi}_2$  with either a hexagonal or a tetragonal structure depended on the ion current density. The temperature rise caused by beam heating and the beam-striking time related to the dose were calculated, and they were responsible for the formation and evolution related to the differently structured  $\text{WSi}_2$  phases.

### 1. Introduction

Metal silicide thin films, which have been studied for more than 20 years because of their potential application in ultra-large-scale integration (ULSI), have been generally fabricated by means of thermally induced or ion-mixing-induced reaction [1, 2] between deposited thin metal films and silicon single crystals. Of the metal silicides, tungsten disilicide is very attractive because of its relatively low resistivity, high thermal stability and unique oxidation capability [3-5].

The properties of  $\text{WSi}_2$  films on silicon wafers depend on the different crystalline structures of  $\text{WSi}_2$ , i.e. the hexagonal structure (C40 with  $a = 4.164 \text{ \AA}$  and  $c = 6.414 \text{ \AA}$ ) usually formed by annealing in the temperature range 400-600 °C or the tetragonal structure (C11b with  $a = 3.211 \text{ \AA}$  and  $c = 7.869 \text{ \AA}$ ) formed by annealing at a temperature of 700 °C or higher [6, 7].

Ion beam synthesis is a promising technique for fabricating silicides, e.g. continuous buried  $\text{CoSi}_2$  [8, 9],  $\alpha\text{-FeSi}_2$  and  $\beta\text{-FeSi}_2$  [10, 11] layers have been formed by high-dose Co and Fe ion implantation into Si single crystals at an elevated Si wafer temperature and post-annealing. In contrast with the conventional ion beam synthesis techniques previously employed, a high current density of various metal ions can be readily extracted from a newly invented metal vapour vacuum arc (MEVVA) ion source [12]. If MEVVA ion implantation were employed to form various metal silicides, the high-current ion beam would certainly heat the Si wafers up to high temperatures and reach the temperatures required for forming various metal silicides by adjusting the current density and dose. Apparently, the MEVVA source provides a possible manufacturing technique which requires only a single implantation step. The feasibility of the MEVVA technique has been verified by our previous study in forming the C54  $\text{TiSi}_2$  phase with a very low resistivity by direct Ti ion implantation [13]. In

this paper, we report the preliminary results of the formation of  $\text{WSi}_2$  fabricated by direct high-current W ion implantation into Si(111) wafers.

## 2. Experimental procedure

Before loading onto a steel sample holder, the p-type Si(111) wafers with a resistivity of 8–13  $\Omega$  cm were cleaned by a routine chemical procedure and then dipped in a dilute HF solution, followed by a rinse in deionized water. The samples were not deliberately cooled during implantation which was carried out in a MEVVA source implanter with a vacuum level of better than  $5 \times 10^{-3}$  Pa. Various current densities of W ion implantation, ranging from 50 to 115  $\mu\text{A cm}^{-2}$ , were performed at an extract voltage of 40 kV and a dose of  $5 \times 10^{17}$   $\text{W cm}^{-2}$ . The ion beam consisted of 8%  $\text{W}^+$ , 34%  $\text{W}^{2+}$ , 36%  $\text{W}^{3+}$ , 19%  $\text{W}^{4+}$  and 3%  $\text{W}^{5+}$ . The samples were implanted with a tilt angle of  $7^\circ$  to avoid the channelling effect.

X-ray diffraction (XRD) measurements were conducted using a D/max-RB diffractometer with a Cu radiation source operated at 40 kV and 80 mA. The implanted W ion profiles were determined by Rutherford backscattering spectrometry (RBS) at a  $165^\circ$  scattering angle with 2.1 MeV He particles.

## 3. Results and discussion

### 3.1. Phase formation of $\text{WSi}_2$

In the sample implanted by W ions with a current density of 50  $\mu\text{A cm}^{-2}$ , no silicide can be observed by XRD. The XRD spectra of two differently structured  $\text{WSi}_2$  phases obtained in the samples implanted with W ions at various current densities are shown in figure 1. When the current density was increased to 65  $\mu\text{A cm}^{-2}$ , a peak of  $d = 2.154$  Å appeared (figure 1(a)), corresponding to the (111) line of hexagonal  $\text{WSi}_2$  [7]. Figure 1(b) reveals that the hexagonal phase of  $\text{WSi}_2$  is completely formed in the sample implanted with W ions at a current density of 75  $\mu\text{A cm}^{-2}$ . As can be seen from figure 1(c), the hexagonal-to-tetragonal phase transformation began to take place when the ion current density was increased to 90  $\mu\text{A cm}^{-2}$ . On implantation at an ion current density of 115  $\mu\text{A cm}^{-2}$ , the tetragonal  $\text{WSi}_2$  phase was formed, which accorded with [14], and coexisted with its hexagonal counterpart (figure 1(d)).

In previous reports the formation of hexagonal  $\text{WSi}_2$  was anticipated on lower-temperature annealing, while the tetragonal structure would be formed at higher temperatures. It had been deduced that a temperature of the order of 550 °C was necessary to initiate the transition from hexagonal  $\text{WSi}_2$  to the tetragonal  $\text{WSi}_2$  [7] and that the tetragonal phase was the only phase present beyond 700 °C, demonstrated by other techniques [6, 7, 15]. In our case, changing the ion current density in MEVVA source implantation corresponds to varying the effective annealing temperature, which in turn induces the formation of  $\text{WSi}_2$  with the corresponding structures. The quantitative calculation of the temperature rise versus ion current density is discussed later in section 3.3.

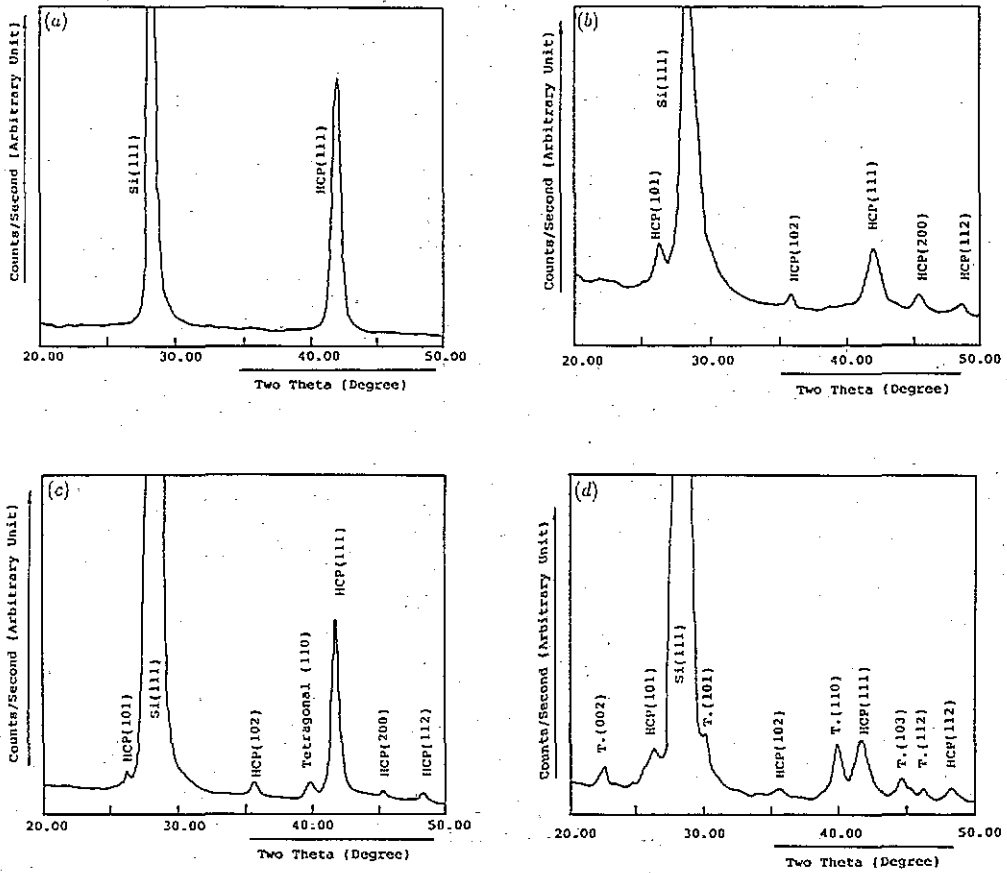


Figure 1. XRD spectra of Si(111) samples implanted with W ions to a dose of  $5 \times 10^{17} \text{ cm}^{-2}$  at various current densities: (a)  $65 \mu\text{A cm}^{-2}$ ; (b)  $75 \mu\text{A cm}^{-2}$ ; (c)  $90 \mu\text{A cm}^{-2}$ ; (d)  $115 \mu\text{A cm}^{-2}$ .

### 3.2. Diffusion of W ions in silicon

The two Rutherford backscattering spectra in figure 2 were obtained from the samples implanted with W ions at two current densities of 65 and  $90 \mu\text{A cm}^{-2}$  at a fixed dose of  $5 \times 10^{17} \text{ cm}^{-2}$ . The spectrum in figure 2(a) for the sample implanted with W ions at a current density of  $65 \mu\text{A cm}^{-2}$  shows that a relatively sharp silicide layer with an average stoichiometry of  $W:Si = 1:2.33$  had been formed at the surface layer, 300 Å thick. When the current density was increased to  $90 \mu\text{A cm}^{-2}$ , the corresponding spectrum in figure 2(b) demonstrates that the W ions had diffused considerably into the depth of Si and the peak W concentration reached an average stoichiometry of  $W:Si = 1:3.4$  within a 300 Å flat distribution and a 400 Å enhanced diffusion layer. The higher the current density, the more W ion diffusion takes place. The Rutherford backscattering spectrum in figure 3 reveals that the W profile extended markedly to a depth of 1000 Å when the current density was increased to  $115 \mu\text{A cm}^{-2}$ . The stoichiometry of  $W:Si$  in the implanted layer was 1:4 and the Si concentration increased deeper into the layer. However, for all the above implanted samples, XRD detected only  $WSi_2$  phases and no other compounds. These results meant that the  $WSi_2$  phase formed directly after implantation was not uniform.

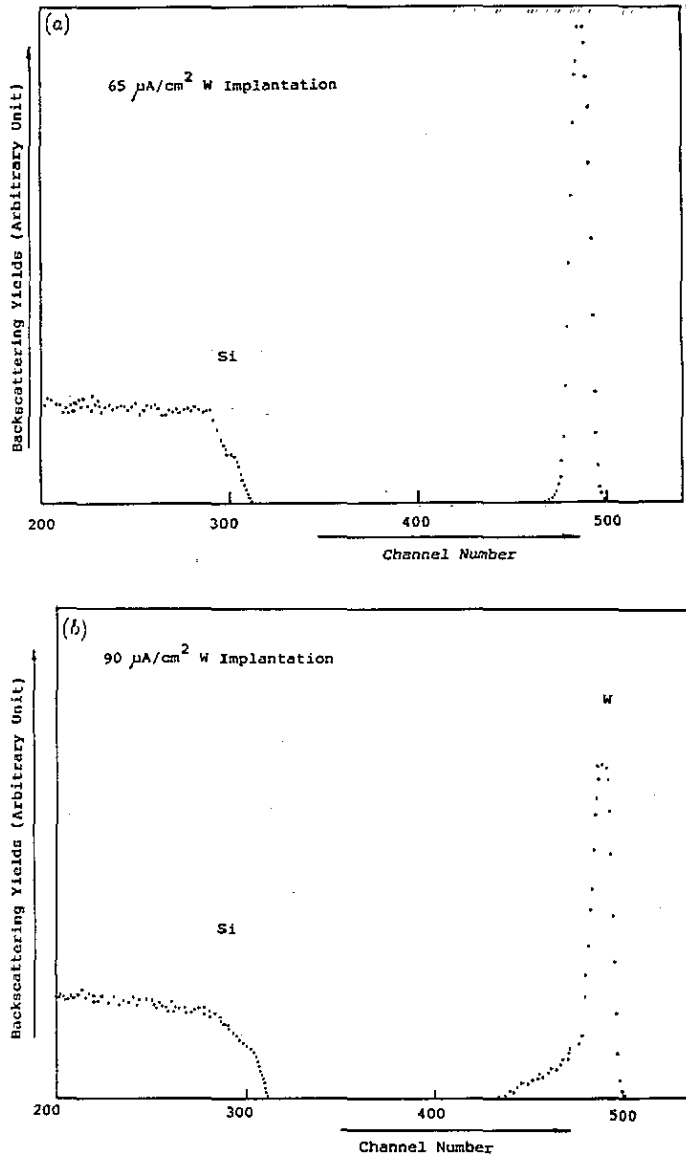


Figure 2. Rutherford backscattering spectra of Si(111) samples implanted with W ions to a dose of  $5 \times 10^{17} \text{ cm}^{-2}$  at two current densities: (a)  $65 \mu\text{A cm}^{-2}$ ; (b)  $90 \mu\text{A cm}^{-2}$ .

### 3.3. Beam-heating effect in MEVVA implantation

Both the x-ray and RBS results indicate that the beam-heating effect plays an important role in determining the uniformity and the crystalline structure of the  $\text{WSi}_2$  formed. The instantaneous temperature rise under ion implantation can be calculated using the expression of Wittkower and Hirvonen [16]:

$$\Delta T(t) = T(t) - T_s = 2P \cos \theta \sqrt{t/k\rho C_p} \text{ (}^\circ\text{C)} \quad (1)$$

where  $T(t)$  ( $^\circ\text{C}$ ) is the instantaneous temperature of the sample surface,  $T_s$  ( $^\circ\text{C}$ ) the average temperature,  $P$  ( $\text{W cm}^{-2}$ ) the instantaneous power density of the ion beam,  $k$

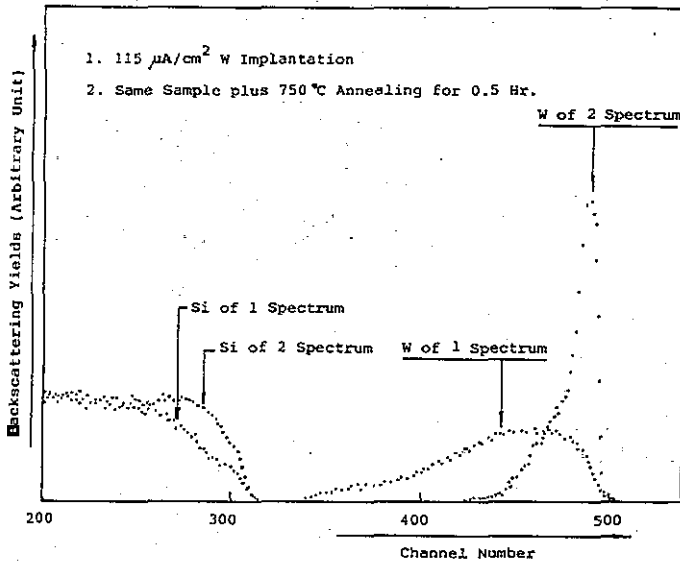


Figure 3. Rutherford backscattering spectra of an Si(111) sample implanted with W ions to a dose of  $5 \times 10^{17} \text{ cm}^{-2}$  at a current density of  $115 \mu\text{A cm}^{-2}$  before (spectrum 1) and after annealing (spectrum 2).

( $\text{W cm}^{-1} \text{ } ^\circ\text{C}^{-1}$ ) the thermal conductivity of the material being implanted,  $C_p$  ( $\text{W s g}^{-1} \text{ } ^\circ\text{C}^{-1}$ ) the specific heat of the material being implanted,  $\rho$  ( $\text{g cm}^{-3}$ ) the density of the material being implanted,  $\theta$  (deg) the tilt angle of implantation and  $t$  (s) the beam striking time.

Under our experimental condition,  $\theta$  is  $7^\circ$ , and the values of  $k$  and  $C_p$  for Si are  $0.84 \text{ W cm}^{-1} \text{ } ^\circ\text{C}^{-1}$  and  $1.58 \text{ W s cm}^{-3} \text{ } ^\circ\text{C}^{-1}$ , respectively. Equation (1) becomes

$$\Delta T(t) = 1.47 J \sqrt{t} \quad (2)$$

where  $J$  ( $\mu\text{A cm}^{-2}$ ) is the instantaneous ion beam current density and  $t$  (min) the beam-striking time.

In order to illustrate explicitly the relationship between the crystalline structure of  $WSi_2$  and the beam-heating effect, the details of  $WSi_2$  phases and the beam-striking times versus various current densities are listed in table 1. In addition, five  $\Delta T(t)$  versus  $t$  curves are given in figure 4 to show the temperature rise process during implantation. For current densities of  $65$  and  $75 \mu\text{A cm}^{-2}$ , the temperature rise is in the same range  $400$ – $600^\circ\text{C}$ , and the beam-striking times are  $22$  min and  $17$  min for figure 4, curve 2 and curve 3, respectively. In both cases, the observation of only a hexagonal phase after implantation coincides with the previously reported results [6]. When the current density is increased to  $90 \mu\text{A cm}^{-2}$ , the beam-striking time is  $10$  min in the temperature range  $600$ – $700^\circ\text{C}$  (figure 4, curve 4), which results in the hexagonal-to-tetragonal phase transition as shown by the (110) line for tetragonal  $WSi_2$  shown in figure 1(d). This result is also in accordance with previous reports.

Unlike the formation of hexagonal  $WSi_2$  in the temperature range  $400$ – $550^\circ\text{C}$  as reported previously, no tungsten silicide was detected when implanting W ions at a current density of  $50 \mu\text{A cm}^{-2}$ , which corresponded to a temperature rise of between  $400$  and  $540^\circ\text{C}$  (figure 4, curve 1). Also, the hexagonal phase remained even when the current density was increased to  $115 \mu\text{A cm}^{-2}$ , which caused the temperature rise to be above  $700^\circ\text{C}$  (figure 4,

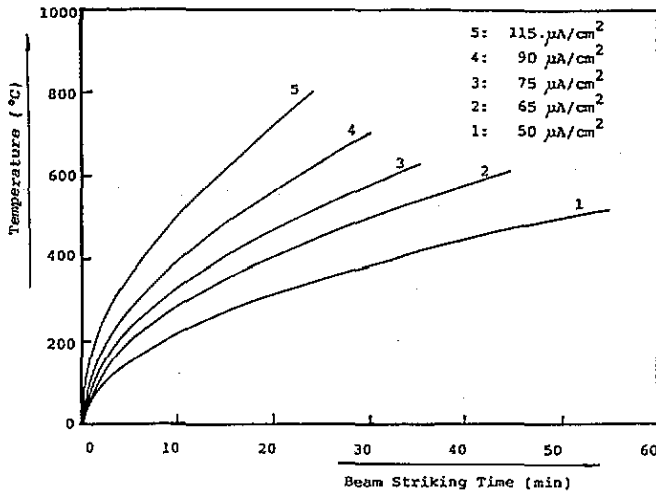


Figure 4. Dependence of the temperature rise on beam-striking time of W ions implanted into Si(111) at various current densities.

Table 1. Different phases of  $\text{WSi}_2$  identified by x-ray diffraction for various W ion current densities: H, hexagonal structure; T, tetragonal structure.

Phases for the following $j$ and $t$				
$50 \mu\text{A cm}^{-2}$	$65 \mu\text{A cm}^{-2}$	$75 \mu\text{A cm}^{-2}$	$90 \mu\text{A cm}^{-2}$	$115 \mu\text{A cm}^{-2}$
54 min	43 min	36 min	31 min	24 min
None	H(111)	H(101) H(102) H(111) H(200) H(112)	H(101) H(102) H(111) H(200) H(112) T(110)	H(101) H(102) H(111) H(112) T(002) T(101) T(110) T(103) T(112)

curve 5). These results can be explained by an insufficient beam-striking time, which was limited by a fixed dose of  $5 \times 10^{17} \text{ cm}^{-2}$ . Naturally, the growth kinetic conditions for metal silicide formation relate to not only the temperature but also the time of interaction between metal and silicon and, in the implantation case, depend on the ion current density as well as the total implantation dose. The beam-striking times for the above two samples were only 25 min and 7 min, respectively, which were too short for the corresponding phase formation or transition to be completed.

From the above explanation in terms of the beam effect and the RBS results, it is necessary to increase the reactive time between W and Si so that a well grown tetragonal  $\text{WSi}_2$  layer with a relatively sharp interface may be formed. For the sample implanted with W ions at a current density of  $115 \mu\text{A cm}^{-2}$ , post-annealing was conducted at  $750^\circ\text{C}$  for 0.5 h in a furnace with a vacuum level of  $3 \times 10^{-3} \text{ Pa}$ . The Rutherford backscattering spectrum 2 in figure 3 shows that, after annealing, a relatively sharp  $\text{WSi}_2$  layer was formed. Meanwhile, as can be seen in the XRD pattern in figure 5, only the diffraction lines from tetragonal  $\text{WSi}_2$  are shown in the annealed sample, indicating that the hexagonal-to-

tetragonal transition was complete. This result can be attributed to an additional reaction between W and Si caused by post-annealing. It is believed that this can also be done by adding a certain amount of implantation dose corresponding to an increase in the beam-striking time. In other words, for high-current ion implantation, not only the beam current density but also the implantation dose should be adjusted for the formation of a uniform metal silicide layer with a relatively sharp interface. The related research on various metal-silicon systems is now currently being undertaken by this group.

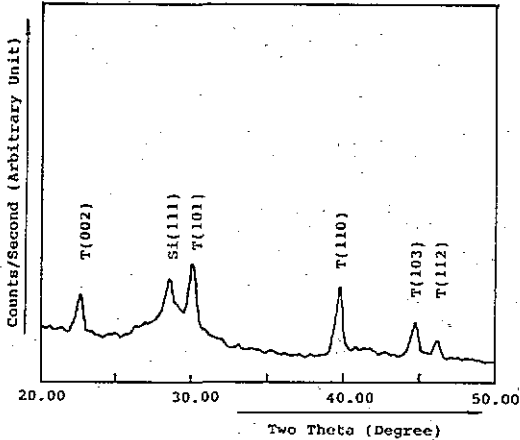


Figure 5. XRD spectrum of an Si(111) sample implanted with W ions at a current density of  $115 \mu A cm^{-2}$  to a dose of  $5 \times 10^{17} cm^{-2}$  and annealed for 30 min at  $750^\circ C$ .

In summary, two differently structured  $WSi_2$  phases can be formed by direct implantation employing the MEVVA ion source. The phase formation of  $WSi_2$  with either a hexagonal or a tetragonal structure closely relates to the ion current density. The calculation of the temperature rise suggests that an effective annealing process with increasing temperature occurs simultaneously during implantation; this is responsible for forming the  $WSi_2$  phases. The above results show the possibility of the application of the MEVVA source in ULSI research and development; however, many more studies are certainly required.

### Acknowledgments

This study is supported by the National Natural Science Foundation of China. The authors are grateful to Mr X J Zhang of Beijing Normal University for his kind help with the implantation.

### References

- [1] Murarka S P 1983 *Silicides for VLSI Application* (New York: Academic)
- [2] Matteson S and Nicolet M A 1983 *Ann. Rev. Mater. Sci.* **13** 339-62
- [3] Tsai M Y, d'Heurle F M, Peterson C S and Johnson R W 1981 *J. Appl. Phys.* **52** 5350
- [4] Nava F, Weiss B Z, Ahn K Y, Smith D A and Tu K N 1988 *J. Appl. Phys.* **64** 354
- [5] Tjong S C and Hsieh I C 1987 *Mater. Res. Bull.* **2** 841
- [6] Murarka S P, Read M H and Chang C C 1981 *J. Appl. Phys.* **52** 7451
- [7] d'Heurle F M, Peterson C S and Tsai M Y 1980 *J. Appl. Phys.* **51** 5976
- [8] White A E, Short K T, Dynes R C, Garno J P and Gibson J M 1987 *Appl. Phys. Lett.* **50** 95
- [9] Heieh Y F, Hull R, White A E and Short K T 1991 *Appl. Phys. Lett.* **58** 122



- [10] Radermacher K, Mantl S, Dieker C and Luth H 1991 *Appl. Phys. Lett.* **59** 2145
- [11] Oostra D J, Vandenhoude D E W, Bulle-Lieuwma C W T and Naburgh E P 1991 *Appl. Phys. Lett.* **59** 1737
- [12] Brown I G, Gavin J E and MacGill R A 1985 *Appl. Phys. Lett.* **47** 358
- [13] Zhu D H, Tao K, Pan F and Liu B X 1993 *Appl. Phys. Lett.* **62** 2356
- [14] Joint Committee on Powder Diffraction Standards 1972 *Powder Diffraction File* (Swathmore, PA: International Center for Diffraction Data), Card 11-195
- [15] Amiotti M, Bellandi E, Borghesi A, Piaggi A, Guizzetti G, Nava F and Queirolo G 1992 *Appl. Phys. A* **54** 181-5
- [16] Wittkower A and Hirvonen J K 1985 *Nucl. Instrum. Methods B* **6** 78